

Azimuthal charged particle correlations as a probe for local strong parity violation in heavy-ion collisions

Ilya Selyuzhenkov for the STAR Collaboration

Indiana University Cyclotron Facility, 2401 Milo B. Sampson Lane, Bloomington, IN 47408, USA

One of the most interesting and important phenomena predicted to occur in heavy-ion collisions is the local strong parity violation. In non-central collisions, it is expected to result in charge separation of produced particles along the system's orbital momentum. I report on results of the charge separation measurement in Au+Au and Cu+Cu collisions at $\sqrt{s_{NN}} = 200$ and 62 GeV with the STAR detector at RHIC based on three-particle mixed harmonic azimuthal correlations. Systematic study of parity conserving (background) effects with existing heavy-ion event generators, and their possible contributions to the observed correlations are also present.

1. Introduction

A heavy-ion collision provides a unique environment to study particle interactions at a very high temperature and extreme density. Among the most important features of the system created in non-central heavy-ion collisions are the strong magnetic field $B \sim 10^{15}$ T ($eB \sim 10^4$ MeV²) [1, 2, 3], and large orbital angular momentum $L \sim 10^5$ [4, 5]. Together with non-uniform particle density and pressure gradient in the overlap area formed by the colliding nuclei (depicted by the color region in Fig. 1), such initial conditions result in a variety of interesting physics phenomena which are currently under study at the Relativistic Heavy Ion Collider (RHIC). Among the most extensively studied is the anisotropic

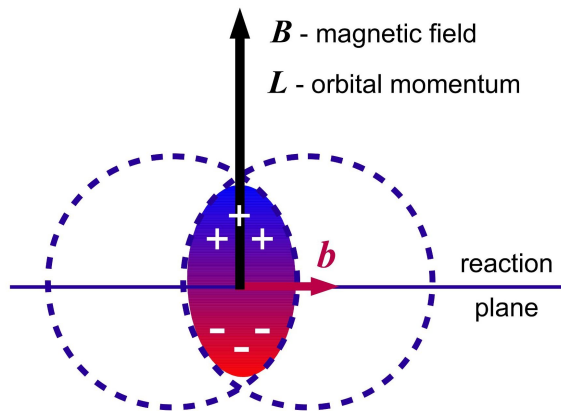


Figure 1: Schematic view of non-central heavy-ion collision. Colliding nuclei (depicted as dashed circles) are moving out-of-list. Magnetic field (B) and system orbital momentum (L) are perpendicular to the reaction plane (plane spanned by the impact parameter, b , and colliding nuclei direction).

transverse flow, which reflects the evolution of initial space anisotropy of particle production in the overlap area into momentum space. This collective effect has been measured at RHIC and SPS (Super Proton Synchrotron) (see [6] and references therein), and the strong elliptic and directed flow observed at RHIC are key measures which indicate the quark-gluon plasma formation in heavy-ion collisions.

Another interesting phenomena predicted to occur in non-central heavy-ion collisions is global polarization and spin alignment [4, 7]. It manifests itself in preferential orientation of the spin of produced particles wrt. the system orbital momentum (perpendicular to the reaction plane as illustrated in Fig. 1). This effect has been recently measured by the STAR Collaboration for strange hyperons (Λ , $\bar{\Lambda}$) and vector mesons (K^{*0} , ϕ), and is experimentally found to be consistent with zero within experimental uncertainties [8, 9].

In this presentation I report on results of the STAR studies of the local strong parity (\mathcal{P}) violation. Experimental evidence for this effect would be an observation of charge separation along the direction of the magnetic field (preferential emission of the same charged particles in the same direction). This effect is illustrated by "+" (positive) and "-" (negative) charge separation in Fig. 1.

The underlying physics of charge separation originates in the fundamental features of the QCD vacuum. The modern understanding of the QCD theory is that its vacuum (gluonic field energy) is periodic vs. so-called Chern-Simons number N_{CS} (related to the topological charge, Q , as $Q = N_{CS}(+\infty) - N_{CS}(-\infty)$) [10], and there exist localized in space and time solutions (topological configurations) which corresponds to the transformation from one local minima to another. Transition between different vacua can be either via tunneling (instanton) or go-over-barrier (sphaleron) (see [3] and references therein). Figure 2 schematically illustrates these transitions. Quark interaction with either of these topo-

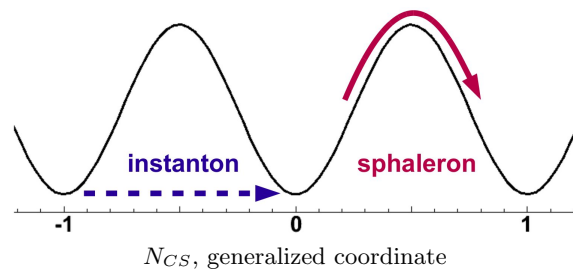


Figure 2: Schematic view of QCD vacuum and its topological transitions from one local minima to another (tunneling via instanton, or go-over-barrier via sphaleron).

logical configurations changes chirality, which is a \mathcal{P} and time reversal odd transition.

At the same time it is experimentally known that \mathcal{P} and CP invariance are (globally) preserved in strong interactions. The evidence comes from neutron electric dipole moment experiments, which put a strong constraint on the possible magnitude of the parity violating parameter [11, 12]: $\theta < 10^{-10}$ (if $\theta \neq 0$, then QCD vacuum breaks \mathcal{P} and CP symmetry).

It was recently argued by Kharzeev *et. al.* [1, 2, 3] that in non-central heavy ion collisions (local) formation of metastable \mathcal{P} -odd domains is not forbidden. Such local strong parity violation can be viewed as a combined result of the following physics effects [3]:

- External magnetic field aligns quark spins along or opposite to its direction. Right-handed quark momentum becomes opposite to the left-handed one.
- Vacuum topological transitions produce a domain with local excess of left or right handed quarks $N_{\text{left}} \neq N_{\text{right}}$ (what corresponds to non-zero topological charge).
- Magnetic field induces electric field which is parallel to it: $E \sim \theta \cdot B$. In this electric field positive and negative charges start to move opposite to each other, which in a finite volume results in charge separation.

Depending on the sign of the domain's topological charge, positively charged particles will be preferentially emitted either along, or in the direction opposite to, the system orbital angular momentum, with negative particles flowing oppositely to the positive particles.

2. Experimental observable

Charge separation can be described by adding \mathcal{P} -odd sine terms to the Fourier decomposition of the particle azimuthal distribution with respect to the reaction plane angle, Ψ_{RP} [13]:

$$\frac{dN_{\pm}}{d\phi_{\alpha}} \propto 1 + 2 \sum_{n=1}^{\infty} v_{n,\pm} \cos n\Delta\phi_{\alpha} + 2a_{\pm} \sin \Delta\phi_{\alpha}, \quad (1)$$

where $\Delta\phi_{\alpha} = \phi_{\alpha} - \Psi_{RP}$ is the particle azimuth relative to the reaction plane, v_n are coefficients accounting for the anisotropic flow (v_1 is called directed, and v_2 is elliptic flow). The a parameters, $a_- = -a_+$, describe the \mathcal{P} -violating effects (in the present study we consider only the first harmonic).

For mid-central collisions at RHIC energies, predicted value for the a parameter is of the order of 1% [1], which is too small to be observed in a single event. The direct, \mathcal{P} -odd, observable $\langle a_{\pm} \rangle$ (average asymmetry over many events) must also yield zero, and the only way to experimentally probe charge asymmetry is to use multi- (two

or more) particle correlations, what limits the measurement to \mathcal{P} -even observables only. This brings a problem of separating (or suppressing) \mathcal{P} -conserving background physics effects in the measurement. Physics backgrounds can be sorted into two different categories: background which produce correlations independent of the reaction plane orientation and those which are reaction plane dependent. To suppress reaction plane independent backgrounds, Voloshin proposed to use the following two particle correlator wrt. the reaction plane [13]:

$$\langle \cos(\phi_{\alpha} + \phi_{\beta} - 2\Psi_{RP}) \rangle = \quad (2)$$

$$= \langle \cos \Delta\phi_{\alpha} \cos \Delta\phi_{\beta} \rangle - \langle \sin \Delta\phi_{\alpha} \sin \Delta\phi_{\beta} \rangle \quad (3)$$

$$= [\langle v_{1,\alpha} v_{1,\beta} \rangle + B_{in}] - [\langle a_{\alpha} a_{\beta} \rangle + B_{out}]. \quad (4)$$

Here B_{in} and B_{out} correspond to the in- and out-of plane background contributions to the correlator, and α, β denote particle charge. Figure 3 illustrates the relation between various azimuthal angles in the laboratory frame and the reaction plane orientation.

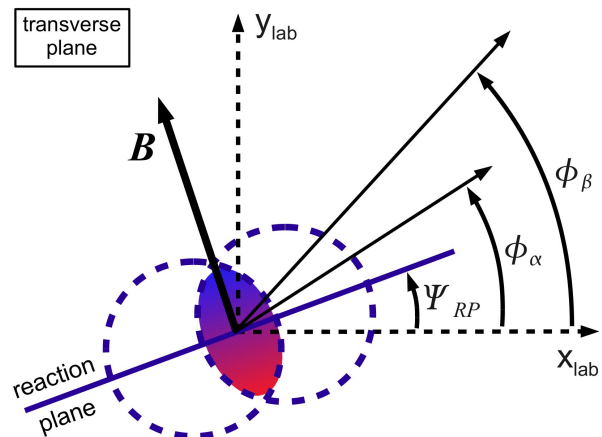


Figure 3: Relation between azimuthal angles of the particle α and β in the laboratory frame and the reaction plane.

The correlator (3) represents the difference between correlations projected onto an axis in the reaction plane and the correlations projected onto an axis that is out-of-plane or perpendicular to the reaction plane. The key advantage of using a difference equation is that it removes all the background correlations among particles α and β that are not related to the reaction plane orientation [14, 15].

3. Expectations for charge correlations

The first estimates [1] of the charge asymmetry predicted a signal of the order of $|a| \sim Q/N_{\pi^+}$, where $Q = 0, \pm 1, \pm 2, \dots$ is the topological charge and N_{π^+} is the positive pion multiplicity in one unit of rapidity. More accurate estimates [2] were found to be close to the same number, of the order of 10^{-2} for mid-central collisions, which corresponds to 10^{-4} for the correlator

$\langle a_\alpha a_\beta \rangle$ (third term in Eq. 4). Without in medium effects, one expects the symmetry between same- and opposite-sign correlations: $\langle a_+ a_+ \rangle = \langle a_- a_- \rangle = -\langle a_+ a_- \rangle > 0$, but in case of heavy ion collisions one needs to account for correlation modification due to particle interaction with the medium. This is similar to the back-to-back suppression of jet-like correlations, and is predicted to result in suppression of opposite sign correlations [2]: $\langle a_+ a_+ \rangle = \langle a_- a_- \rangle \gg -\langle a_+ a_- \rangle$. The correlator $\langle a_\alpha a_\beta \rangle$ should follow (a typical for any kind of correlations due to clusters) $1/N_{ch}$ dependence (N_{ch} is the charge multiplicity). Local parity violation is a non-perturbative effect and the main contribution should come from particles which have transverse momentum smaller than 1 GeV/c [2], with correlation width of the order of one unit in rapidity (typical size of the \mathcal{P} -odd domain is about 1 fm).

4. Measurement technique

The reaction plane orientation is not known a priori in the experiment, and it needs to be reconstructed from particle azimuthal distributions [16]. For that reason instead of measuring the two particle correlator wrt. the reaction plane (2), we evaluate the three particle correlator, where the third particle, c , gives an estimate of the reaction plane. Such a three particle correlator can be related to the correlator (2) by the following equation:

$$\langle \cos(\phi_\alpha + \phi_\beta - 2\psi_{RP}) \rangle = \langle \cos(\phi_\alpha + \phi_\beta - 2\phi_c) \rangle / v_{2,c}. \quad (5)$$

Here $v_{2,c}$ is an elliptic flow value of the third particle c , and it accounts for the finite resolution in our estimate of the reaction plane angle [15, 16, 17]. Equation 5 assumes that particle c is correlated with particles α and β only via common correlation to the reaction plane. This third particle further complicates experimental data analysis, since it potentially adds to the measured values of the correlator (5) some background contributions from genuine 3-particle correlations. These contributions are discussed in Sec. 8.

5. Experimental setup

The results presented here are based on 14.7M Au+Au and 13.9M Cu+Cu collisions at the incident energies $\sqrt{s_{NN}}=200$ GeV, and 2.4M Au+Au and 6.3M Cu+Cu events at $\sqrt{s_{NN}}=62$ GeV. Collisions were recorded with the STAR detector during the 2004 and 2005 runs. Charged particle tracks were reconstructed in a cylindrical and azimuthally symmetric Time Projection Chamber (TPC) [18, 19]. A minimum bias trigger was used during data-taking with offline collision vertex cut of 30 cm along the beam line from the center of the main TPC.

The correlations are reported in the pseudorapidity region $|\eta| < 1.0$ with particle momentum $0.15 < p_t <$

2.0 GeV/c (unless stated otherwise). Standard STAR track quality cuts are applied [20]. The Large elliptic flow measured at RHIC [21] is used to estimate the reaction plane from particle distributions in the main TPC and two Forward Time Projection Chambers (FTPC) [22]. The latter cover pseudorapidity intervals $2.7 < |\eta| < 3.9$. In the most forward direction, STAR has two Zero Degree Calorimeter - Shower Maximum Detectors (ZDC-SMD) [23, 24]. ZDC-SMDs are sensitive to the directed flow of neutrons in the beam rapidity regions, which is used for the reaction plane reconstruction.

6. Understanding detector effects

Detector effects have been corrected with recentering procedure [16]. Corrections are applied run-by-run, separately for positive and negative particles, for each centrality bin, and as a function of particle pseudorapidity and transverse momentum. The validity of the recentering method was verified by calculating three-particle cumulants according to [14, 25].

Figure 4 shows three-particle correlator $\langle \cos(\phi_\alpha + \phi_\beta - 2\phi_c) \rangle$ as a function of reference multiplicity (measured charge multiplicity in $|\eta| < 1$) in Au+Au collisions at $\sqrt{s_{NN}}=200$ GeV (a) before and (b) after correcting for detector effects. The signal is scaled by the reference

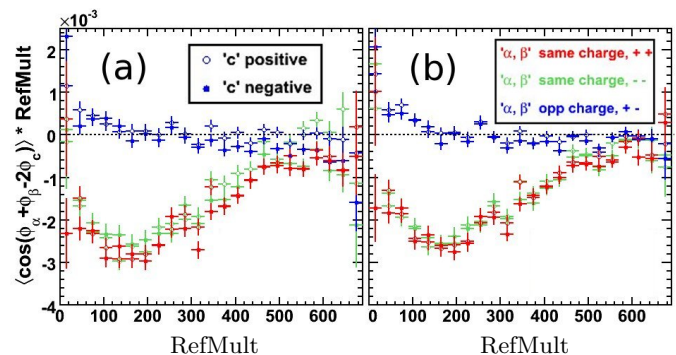


Figure 4: $\langle \cos(\phi_\alpha + \phi_\beta - 2\phi_c) \rangle$ as a function of reference multiplicity for different charge combinations [20]: (a) before corrections for acceptance effects, and (b) after corrections. In the legend the signs indicate the charge of particles α , β , and c .

multiplicity to better indicate the acceptance effects for central collisions. All the differences which do not depend on the relative charge of α and β disappear after the acceptance correction. We have performed several additional checks to ensure that the signal is not due to detector effects:

- Distortions in the track momenta due to the charge buildup in the STAR Time Projection Chamber (TPC) at high accelerator luminosity. Results obtained from RHIC Run II (a low luminosity run), and those from Run IV divided into high and low

luminosity events, yield the same signal within statistical uncertainties.

- Signal dependence on reconstructed position of the collision vertex along the beam line has been checked, and no dependence has been found.
- Displacement of track hits when it passes the TPC central membrane. The correlator (5) has been calculated using only particles with the entire track in one of the different half-barrels of the TPC. Corrected for the signal dependence on the track separation in pseudorapidity, results are found to be consistent with those obtained before introducing the rapidity separation.
- Feed-down effects from non-primary tracks (i.e. resonance decay daughters) have been studied via cuts on track distance of closet approach (dca). Results for $dca < 1$ cm and $dca < 3$ cm are found to be consistent within statistical errors.
- Electron contribution to the measured signal has been checked via specific energy loss (dE/dx) in the volume of the TPC and found to be negligible. This check was done to test whether the signal was due to hadron production, or lepton production.
- Studied a correlator similar to (5) but with the reaction plane angle rotated by $\pi/4$. This new correlator should only deviate from zero due to detector effects. It was found to be consistent with zero within statistical errors.
- Variation depending on the charge of the third particle used to reconstruct the reaction plane and changes of the STAR magnetic field polarity. The variations does not change the observed signal.

Our conclusion from a number of tests performed is that detector effects are not responsible for the observed correlations.

7. Testing sensitivity to 2-particle correlations wrt. the reaction plane

Figure 5(a) compares the three-particle correlations $\langle \cos(\phi_\alpha + \phi_\beta - 2\phi_c) \rangle$ obtained for different charge combinations, as a function of centrality, when the third particle is selected from the main TPC (solid symbols) with when it is selected from the Forward TPCs (open symbols). Elliptic flow data have been taken from Ref. [26, 27].

Assuming that the second harmonic of the third particle is correlated with the first harmonic of the first two particles via a common correlation to the reaction plane, the correlator should then be proportional to the elliptic flow of the third particle. Figure 5(b) shows very good agreement between the same charge correlations obtained

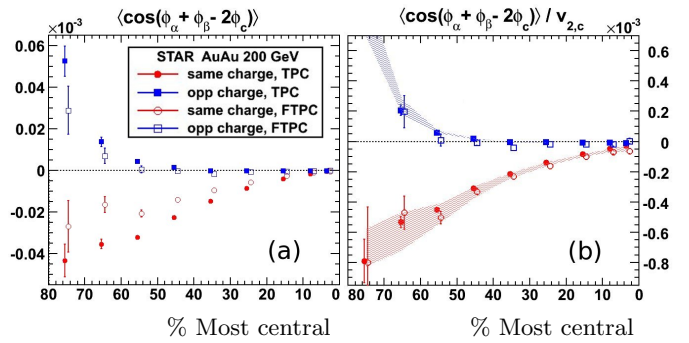


Figure 5: (a) $\langle \cos(\phi_\alpha + \phi_\beta - 2\phi_c) \rangle$ obtained by selecting the third particle from the main TPC and the Forward TPCs [20]. (b) $\langle \cos(\phi_\alpha + \phi_\beta - 2\phi_c) \rangle$ after scaling by the flow of the third particle. The shaded areas represent the systematic uncertainty from $v_{2,c}$ scaling.

with the third particle in the TPC and FTTPC regions, which supports for such correlations the assumption of Eq. 5. The opposite charge correlations are small in magnitude and with current statistics it is difficult to conclude on validity of the same assumption. Results obtained with the event plane reconstructed with ZDC-SMD are consistent with those shown in Fig. 5(b), though the statistical errors on ZDC-SMD results are about 5 times larger.

Agreement between TPC, FTTPC, and ZDC SMD results give us a confidence that 3-particle correlation that we measure are indeed sensitive to the 2-particle correlations wrt. the reaction plane.

8. Modeling physics backgrounds

Figure 6 shows the correlator (5) for Au+Au collisions at $\sqrt{s_{NN}}=200$ GeV. Blue symbols and lines mark opposite-charge correlations, and red are same-charge. Star symbols represent the STAR data, with shaded area reflecting the uncertainty due to v_2 scaling. Other symbols in Fig. 6 show possible background two particle correlations wrt. the reaction plane estimated from various Monte-Carlo event generator with true reaction plane:

- HIJING [28] with default, quenching-off setting: with (triangles), and without (diamonds) v_2 -afterburner. Elliptic flow is added by "shifting" method [16], with v_2 values consistent with STAR measurements at the given centrality.
- UrQMD [29] with default setting (circles).
- MEVSIM [30] Monte-Carlo simulations (squares). MEVSIM tests resonance (ϕ , Δ , ρ , ω , and K^*) contribution with realistic elliptic flow pattern.

Thick solid lines in Fig. 6 indicate genuine three particle correlations from HIJING (corresponding estimates from UrQMD are about factor of two smaller). HIJING three

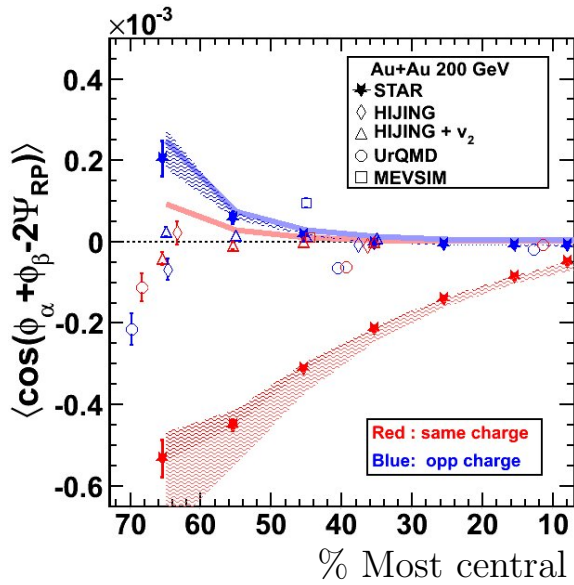


Figure 6: Comparing correlator (5) from STAR data [20] vs. various physics background event generators in Au+Au collisions at $\sqrt{s_{NN}} = 200$ GeV. None of the generators can reproduce same-charge correlations.

particle correlations produce data-like opposite-sign signal (compare blue line with blue stars in Fig. 6), which may indicate dilution of the opposite-sign signal with effects not related to the reaction plane orientation.

Figure 6 shows that no generator gives qualitative agreement with the data, though they produce non-zero correlations. These models do not match the correlations for $\langle \cos(\phi_\alpha - \phi_\beta) \rangle$ that are seen in the data either, which points to the need for better modeling of two-particle correlations to give quantitatively meaningful comparisons for correlator (5). Other background effects studied are (see for details [20]):

- Correlations from processes in which particles α and β are products of a cluster (e.g. resonance, jet, di-jets) decay, and the cluster itself exhibits elliptic flow or decays (fragments) differently when emitted in-plane compared to out-of-plane
- Jets as potential source of reaction-plane dependent background since their properties may vary with respect to the reaction plane.
- Cluster formation, which plays an important role in multiparticle production at high energies, and may account for production of a significant fraction of all particles.
- Directed flow, which on average is zero in a symmetric pseudorapidity interval, but can contribute to the correlator (5) via flow fluctuations (see the first term in Eq. 4).
- Effect of global polarization (discussed in the introduction), which produce polarized secondary par-

ticles along the direction of the system's angular momentum.

From our studies we conclude that none of the background effects listed above can be responsible for the same-sign correlations shown in Fig. 6.

9. Results

Figure 7 shows correlator (5) in Au+Au and Cu+Cu collisions at $\sqrt{s_{NN}} = 200$ GeV. The correlations are

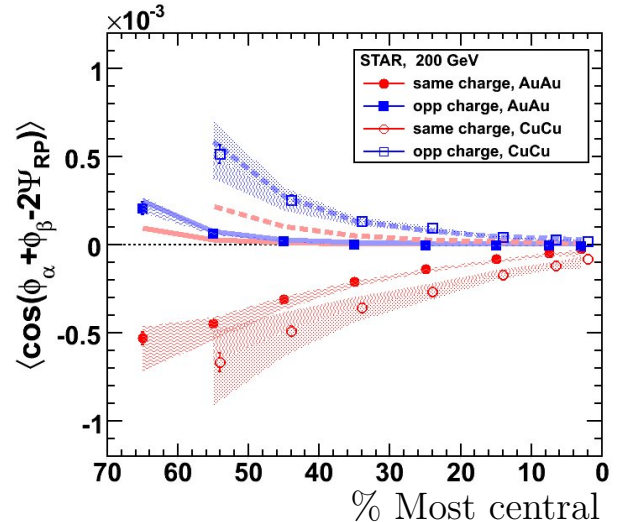


Figure 7: Correlator (5) in Au+Au and Cu+Cu collisions at $\sqrt{s_{NN}} = 200$ GeV [20]. The shaded band indicates uncertainty associated with v_2 scaling. Thick solid (Au+Au) and dashed (Cu+Cu) lines represent HIJING estimates for possible non-reaction-plane dependent contribution from many-particle correlations.

weaker in more central collisions compared to more peripheral collisions, which partially can be attributed to dilution of correlations which occurs in the case of particle production from multiple sources. The correlations in Cu+Cu collisions (open symbols), appear to be larger than the correlations in Au+Au (solid symbols) for the same centrality of the collision. One reason for this difference may be the difference in number of participants (or charge multiplicity) in Au+Au and Cu+Cu collisions at the same centrality. The local \mathcal{P} -violation signal is expected to have approximately $1/N_{ch}$ dependence, and at the same centrality of the collision the multiplicity is smaller in Cu+Cu collisions compared to Au+Au. The difference in magnitude between same and opposite charge correlations is considerably smaller in Cu+Cu than in Au+Au, qualitatively in agreement with the scenario of stronger suppression of the back-to-back correlations in Au+Au collisions.

Figure 8(a) shows the dependence of the correlator (5) on the difference in pseudorapidities of two particles, $|\eta_\alpha - \eta_\beta|$, for 30-50% centralities, while Fig. 8(b) shows

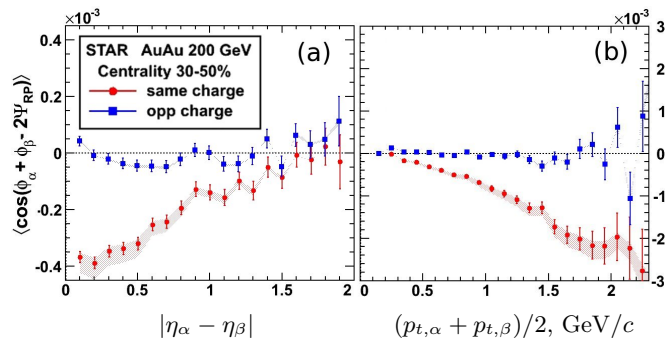


Figure 8: Au+Au at 200 GeV [20]. The correlations dependence on (a) pseudorapidity separation, $|\eta_\alpha - \eta_\beta|$, and (b) on $(p_{t,\alpha} + p_{t,\beta})/2$ for centrality 30-50%. The shaded band indicates uncertainty associated with v_2 scaling.

its dependence on the sum of the transverse momentum magnitudes (without upper p_t cut) for the same centrality region. The correlations have a typical hadronic width of about one unit of pseudorapidity, but we do not observe them to be concentrated in the low p_t region as naively might be expected for \mathcal{P} -violation effects.

Other results, in particular for collisions at $\sqrt{s_{NN}}=62.4$ GeV, correlation scaling with number of participants, and their dependence on transverse momentum difference, can be found in [20].

10. Summary

Formation of local \mathcal{P} -odd domains has been predicted in nuclear collisions [1]. This effect should result in charge separation along the orbital momentum of the system created in non-central heavy-ion collisions. The STAR measurements of 3-particle azimuthal correlations in Au+Au and Cu+Cu collisions at $\sqrt{s_{NN}}=200$ and 62 GeV reveal non-zero signal. Measured 3-particle azimuthal correlations are directly sensitive to local strong parity violation, but susceptible to contributions from \mathcal{P} -conserving backgrounds. So far we could not explain the observed same sign correlations, and data can not be describe with any of the existing Monte-Carlo event generators of the heavy-ion collisions. At the same time, qualitatively the data agrees with predictions for local \mathcal{P} -violation (though the signal persists to higher transverse momentum than expected). The presented measurements demand detailed theoretical calculations of the \mathcal{P} -violating signal and backgrounds to make a definitive statement about possible local strong \mathcal{P} -violation in heavy ion collisions.

References

[1] D. Kharzeev, Phys. Lett. B **633**, 260 (2006).
 [2] D. E. Kharzeev, L. D. McLerran and H. J. Warringa, Nucl. Phys. A **803**, 227 (2008).

[3] K. Fukushima, D. E. Kharzeev and H. J. Warringa, Phys. Rev. D **78**, 074033 (2008).
 [4] Z. T. Liang and X. N. Wang, Phys. Rev. Lett. **94**, 102301 (2005) [Erratum-ibid. **96**, 039901 (2006)].
 [5] J. H. Gao, S. W. Chen, W. t. Deng, Z. T. Liang, Q. Wang and X. N. Wang, Phys. Rev. C **77**, 044902 (2008).
 [6] S. A. Voloshin, A. M. Poskanzer and R. Snellings, arXiv:0809.2949 [nucl-ex].
 [7] S. A. Voloshin, arXiv:nucl-th/0410089.
 [8] B. I. Abelev *et al.* [STAR Collaboration], Phys. Rev. C **76**, 024915 (2007).
 [9] B. I. Abelev *et al.* [STAR Collaboration], Phys. Rev. C **77**, 061902 (2008).
 [10] D. Diakonov, arXiv:0906.2456 [hep-ph].
 [11] M. Pospelov and A. Ritz, Phys. Rev. Lett. **83**, 2526 (1999).
 [12] C. A. Baker *et al.*, Phys. Rev. Lett. **97**, 131801 (2006).
 [13] S. A. Voloshin, Phys. Rev. C **70**, 057901 (2004).
 [14] N. Borghini, P. M. Dinh and J. Y. Ollitrault, Phys. Rev. C **66**, 014905 (2002).
 [15] J. Adams *et al.* [STAR Collaboration], Phys. Rev. Lett. **92**, 062301 (2004).
 [16] A. M. Poskanzer and S. A. Voloshin, Phys. Rev. C **58**, 1671 (1998).
 [17] N. Borghini, P. M. Dinh and J. Y. Ollitrault, Phys. Rev. C **64**, 054901 (2001).
 [18] K. H. Ackermann *et al.* [STAR Collaboration], Nucl. Instrum. Meth. A **499**, 624 (2003).
 [19] M. Anderson *et al.*, Nucl. Instrum. Meth. A **499**, 659 (2003).
 [20] B. I. Abelev *et al.* [STAR Collaboration], arXiv:0909.1717 [nucl-ex].
 [21] K. H. Ackermann *et al.* [STAR Collaboration], Phys. Rev. Lett. **86**, 402 (2001).
 [22] K. H. Ackermann *et al.*, Nucl. Instrum. Meth. A **499**, 713 (2003).
 [23] J. Adams *et al.* [STAR Collaboration], Phys. Rev. C **73**, 034903 (2006).
 [24] C. Adler, *et al.*, Nucl. Instrum. Meth. A **461**, 337 (2001); STAR ZDC-SMD proposal, STAR Note SN-0448 (2003).
 [25] I. Selyuzhenkov and S. Voloshin, Phys. Rev. C **77**, 034904 (2008).
 [26] J. Adams *et al.* [STAR Collaboration], Phys. Rev. C **72**, 014904 (2005).
 [27] S. A. Voloshin [STAR Collaboration], J. Phys. G **34**, S883 (2007).
 [28] M. Gyulassy and X.-N. Wang, Comput. Phys. Commun. **83**, 307 (1994); X.N. Wang and M. Gyulassy, Phys. Rev. D **44**, 3501 (1991).
 [29] S. A. Bass *et al.*, Prog. Part. Nucl. Phys. **41**, 255 (1998) [Prog. Part. Nucl. Phys. **41**, 225 (1998)].
 [30] R. L. Ray and R. S. Longacre, arXiv:nucl-ex/0008009.